

Nonlocal Co-occurrence for Image Downscaling

Sanjay Ghosh

Abstract—Image downscaling is one of the widely used operations in image processing and computer graphics. It was recently demonstrated in the literature that kernel-based convolutional filters could be modified to develop efficient image downscaling algorithms. In this work, we present a new downscaling technique which is based on kernel-based image filtering concept. We propose to use pairwise co-occurrence similarity of the pixelpairs as the range kernel similarity in the filtering operation. The co-occurrence of the pixel-pair is learned directly from the input image. This co-occurrence learning is performed in a neighborhood based fashion all over the image. The proposed method can preserve the high-frequency structures, which were present in the input image, into the downscaled image. The resulting images retain visually-important details and do not suffer from edge-blurring artifact. We demonstrate the effectiveness of our proposed approach with extensive experiments on a large number of images downscaled with various downscaling factors.

Index Terms—Image downscaling, kernel filtering, co-occurrence similarity.

I. INTRODUCTION

Display technology is evolving at an exponential rate. It has brought a substantive increase in display devices offering a wide range of image resolutions (e.g., computer monitors, laptop computer screens, personal digital assistants, mobile phones, i-phones, i-pad etc.). In recent days, we rarely view a photo at its original resolution. Instead, it is instantly reduced from its original multi-megapixel size to much smaller dimensions to be viewed on a camera viewfinder, on a computer/mobile screen, or on the web. To convert images with different resolutions (as two devices may have different display dimensions), it is desirable to develop efficient image downscaling and upsampling (super-resolution) techniques. The goal of image downscaling is to produce a lower resolution image by removing pixels while preserving the original image content as much as possible [1], [2], [3], [4], [5]. In addition to the conversion between different image sizes, image downscaling is also used in image coding.

S. Ghosh is with the Department of Radiology and Biomedical Imaging, University of California San Francisco, USA. The work was primarily done during the period when he was a Visiting Scholar at the University of Iowa, USA, and then a Postdoctoral Scholar at the Pennsylvania State University, USA.

There, downscaling is performed before compression step, and then the missing pixels are interpolated after decompression. In the similar direction, the downscaling of frames are performed in SD/HD video coding. However, researchers are yet to draw a substantial attention towards developing efficient algorithms for image downscaling.

Most of the existing downscaling algorithms perform some form of linear filtering on the image. In particular, the filtering is performed using convolution (with a kernel) before subsampling and subsequent reconstruction, following the sampling theorem [6], [7], [8]. The key objective in these works was to minimize the aliasing artifacts. However, the downscaled images obtained using these strategies are usually over-smoothed. Sometimes the perceptually important details and features cannot be retained. This is primarily because of the non-adaptive nature of the filtering kernel, which is independent of the image content. The same phenomenon is observed in more recent image interpolation techniques [9], [10], [11], [12]. Motivated by the working principle of bilateral filtering [13], the authors in [14] proposed to adapt the kernel shapes to local image patches. We note that bilateral filtering is an example of kernel filtering [15], [16]. Recently, another kernel based method was introduced in [2], where a bilateral-like similarity measure was used in the kernel filtering process. We note that kernel filtering is routinely used in various image quality enhancement tasks including smoothing [17], [18], denoising [19], [20], sharpening [21], inpainting [22], flash/no-flash denoising [23], low-light imaging [24], single photon imaging [25] etc. In this work, we explore the capacity of kernel filtering for image downscaling.

In this paper, we present a downscaling algorithm which is built on the idea of kernel filtering. We introduce a new measure for the range similarity in the filtering step. However, the algorithmic complexity of the proposed method is only linear to the number of input pixels. It does not depend on the kernel size. Being a simple kernel filtering operation, the overall algorithm is simple and could be efficiently implemented on todays hardware.

Organization. The rest of the paper is organized as follows. We present a review of the literature on image downscaling in Section II. The proposed downscaling algorithm is described in Section III, where we also provide a complexity analysis of it. In Section IV, we

report several experiments, exhibiting very competitive results. To demonstrate the effectiveness of our proposal, we performed exhaustive downscaling experiments with a wide range of image classes and different downscaling factor. Finally, we conclude in Section V.

II. RELATED WORK

The classical techniques for image downscaling were originated from the idea of sampling theory [6]. The main streamline of these techniques is to - first filter the image to blur the edges and then subsample the intermediate image (as per the desirable factor) to obtain the final downscaled image. The purpose of applying this lowpass filter is to prevent aliasing in the downscaled image. Finding a suitable lowpass filter along with its kernel parameters remains to be a prominent question for further research in this direction. An alternative approach for image downscaling without filtering is to construct the downscaled image by directly optimizing some form of proximity (similarity measure) between the original and downscaled images. We now present a detailed review of the literature on image downscaling algorithms. In doing so, we group them into two classes depending on whether they are - filtering based or optimization based.

A. Filtering based methods

The key step in most of the traditional algorithms is kernel filtering which aims to suppress the high frequency components in order to avoid aliasing artifacts in the downscaled image [7], [8]. The elementary filters are - box, bicubic, and Lanczos filter [7]. These simple kernel filtering methods fail to preserve edges; thus the downscaled image suffers from over-smoothing artifacts [26]. To retain some of the important details in the downscaled images, authors in [27] proposed a sophisticated kernel filter design. To reduce ringing and over-smoothing artifacts, authors in [10] applied interpolation on image downscaling by adding an extra construction step. A joint bilateral filtering based approach was introduced in [14]. For each output pixel, a suitable filter kernel was adaptively estimated by considering both spatial and color variances of the local region around that pixel. Thus, in contrast to pure segmentation, each input pixel exhibits a weighted contribution to each of the output pixels. Additional care was taken to avoid excessive deformation of the input image and smooth edges. Another joint bilateral filtering based method was proposed in [2] where the range kernel of the bilateral filter favors differences in local pixel neighborhoods. The similarity between two pixels are evaluated in such a way that the high-frequency details are preserved in the downscaled image. The core

idea is based on information theoretic intuition that a piece of data deviating from its neighbors usually contains more valuable information. Moreover, it is believed that the human visual system [28] is more sensitive to such piece of information in an image. This fast downscaling algorithm [2] was particularly suited for large images and videos.

B. Optimization methods

There are approaches which model image downscaling as an optimization problem. The downscaling problem was formulated to maximize the structural similarity index (SSIM) between the input and corresponding downscaled image [1]. The solution leads to a non-linear filter, which computes local luminance and contrast measures on the input image and a smoothed version of it. The global optimization framework could be able to render most of fine details. However, the spatial distribution of pixels within each patch is usually not considered in the SSIM index computation. Therefore, this technique [1] sometimes fails to handle structured patterns, thus resulting in aliasing artifacts. An interpolation-dependent downscaling method was proposed in [29] where the objective of the optimization was set to minimize the sum of square errors between the input image and the one interpolated from the corresponding downsampled image. The problem of downscaling was posed as a L_0 regularized optimization in [30]. It consists of two L_0 priors. One of the priors was intended to enforce the fact that there is an inverse square proportionality between the number of edge pixels of the downscaled image and the downscaling factor. Another prior was used to minimize the sparsity of the downsampling matrix. Image downscaling was performed by remapping high frequencies to the representable range of the downsampled spectrum in [31]. The input image was first decomposed into a set of spatially-localized non-harmonic waves; and then the frequency remapping was modeled as an optimization problem.

III. PROPOSED APPROACH

The proposed convolutional filter based method determines the filter weights such that important details (pixel-pair) are retained in the processed/output image. Similar to [2], we first construct an image of the desired dimension by performing box filtering, followed by Gaussian convolution. We refer this intermediate image as guide image.

Suppose the dimension of the input image f is $M \times N$. For simplicity, let us assume that we are interested in $d \times d$ folded downscaling. Thus the dimension of the downscaled image g is $m \times n$, where $m = M/d$ and

$n = N/d$. In general, a $d \times d$ folded downscaling means that each pixel in g represents a patch of size $d \times d$ in the input image f .

In the box filtering step, we perform an arithmetic averaging of all the pixels in each patch and assign that value as the intensity of downscaled intermediate image (of size $m \times n$). This filtering operation is the step where we obtain a crude estimate of the downscaled image. In the subsequent steps, we refine the pixel values using kernel filtering. Let the intermediate image after box filtering be referred as f_d . The output image g of size $m \times n$ is given by:

$$g(\mathbf{i}) = \frac{\sum_{\mathbf{j} \in \Omega(\mathbf{i})} f(\mathbf{j}) C(f_d(\mathbf{i}), f(\mathbf{j}))}{\sum_{\mathbf{j} \in \Omega(\mathbf{i})} C(f_d(\mathbf{i}), f(\mathbf{j}))}, \quad (1)$$

where $C(f_d(\mathbf{i}), f(\mathbf{j}))$ is the co-occurrence frequency of the intensity pair $(f_d(\mathbf{i}), f(\mathbf{j}))$ in the input image f . Note that $f_d(\mathbf{i})$ is the intensity level of the intermediate guide image (which could have non-integer values as well). For using the co-occurrence frequency we round-off $f_d(\mathbf{i})$ to nearest integer. The two-dimensional neighborhood in (1) is $\Omega(\mathbf{i}) = \mathbf{i} + \Omega_d$, where $\Omega_d = [-d, d]^2$. We note that this neighborhood Ω_d is with respect to the input image f . Therefore the filtering operation in (1) is not similar to those traditional kernel filtering on images. Instead, this can be considered as a special type of guided filtering where the pixel intensities in f_d is updated using one particular neighborhood similarity of f .

A. Nonlocal Co-occurrence

The pair-wise co-occurrence in (1) is computed solely from the input image. We define co-occurrence similarity as following:

$$C(a, b) = \sum_{\mathbf{i}} \sum_{\mathbf{j} \in \mathcal{S}(\mathbf{i})} [f(\mathbf{i}) = a][f(\mathbf{j}) = b], \quad (2)$$

where $[\cdot]$ equals 1 if the expression inside the brackets is true and 0 otherwise. The neighborhood in (2) is $\mathcal{S}(\mathbf{i}) = \mathbf{i} + \mathbb{S}$, where $\mathbb{S} = [-k, k]^2$. Similar to the rationale in [2], we set, $k \geq d$. For simplicity, we assume that the intensities are rounded off to nearest integer. For a 8-bit image, the possible values of a and b are $\{0, 255\}$. We note that $C(\cdot, \cdot)$ stores all co-occurrence pixel intensity-pair across the image over the neighborhood \mathbb{S} . In other words, $C(\cdot, \cdot)$ captures the co-occurrence profile of the original image which is parameterized by k . We refer h as the nonlocal co-occurrence matrix of the input image. The term ‘‘nonlocal’’ is to indicate the fact that we compute the cumulative co-occurrence of each possible pair (a, b) throughout the whole image over restricted neighborhood \mathbb{S} of size $(k \times k)$ around each pixel in the input image. We refer this step of our proposal as *co-occurrence learning*.

Algorithm 1: Co-occurrence learning.

Input: Input image f of size $(M \times N)$;
 Neighborhood parameter k .
Output: Co-occurrence profile C of size (256×256) .

```

1 Set  $C$  as a zero-matrix of size  $(256 \times 256)$ 
2 for  $\mathbf{i} = 1, \dots, (M \times N)$  do
3    $a = \lfloor f_d(\mathbf{i}) \rfloor$  %  $\lfloor \cdot \rfloor$  stands for round-of
   operation
4   for  $\mathbf{j} \in \mathcal{S}(\mathbf{i})$  do
5      $b = \lfloor f(\mathbf{j}) \rfloor$ 
6      $C(a, b) = C(a, b) + 1$ 
7   end
8 end
```

Algorithm 2: Kernel filtering .

Input: Input image f of size $(M \times N)$;
 intermediate image f_d of size $(m \times n)$;
 co-occurrence profile C of size (256×256) .
Output: Downscaled image g of size $m \times n$.

```

1 for  $\mathbf{i} = 1, \dots, (m \times n)$  do
2   Set  $P = 0$  and  $Q = 0$ 
3    $a = \lfloor f_d(\mathbf{i}) \rfloor$  %  $\lfloor \cdot \rfloor$  stands for round-of
   operation
4   for  $\mathbf{j} \in \Omega(\mathbf{i})$  do
5      $b = \lfloor f(\mathbf{j}) \rfloor$ 
6      $w = C(a, b)$  % obtained from
     Algorithm 1
7      $P = P + wf(\mathbf{j})$ 
8      $Q = Q + w$ 
9   end
10   $g(\mathbf{i}) = P/Q$ 
11 end
```

B. Computation Complexity

The proposed technique consists of three steps:

- (i) Box filtering.
- (ii) Learning the co-occurrence profile (**Algorithm 1**).
- (iii) Kernel filtering (**Algorithm 2**).

For completeness, we provide a computation complexity analysis in terms of input pixels $(M \times N)$, downscaling factor d , and model parameter k . It was shown in [32] that box filtering of an image can be performed at constant time complexity (independent of the kernel width). So, the filtering of an image of $(M \times N)$ pixels would require $O(MN)$ computations.

In the co-occurrence learning step in Algorithm 1, we need to perform $O(k^2)$ comparisons for each pixel in

the input image. So the total complexity is $O(MNk^2)$. Finally, there are $O(d^2)$ computations for each pixel in the intermediate image as reported in Algorithm 2. The intermediate image contains total $(MN)/d^2$ pixels. The overall computations required for downscaling an image of $(M \times N)$ pixels by a factor of d is:

$$\begin{aligned} &= O(MN) + O(MNk^2) + \frac{MN}{d^2}O(d^2) \\ &= O(MN) + O(MNk^2) + O(MN) \quad (3) \\ &= O(MNk^2). \end{aligned}$$

Alternatively, the per-pixel complexity with reference to input image is $O(k^2)$. In most experiments, we used $k = d$; therefore the per-pixel computation is $O(d^2)$. We note that [2] has very similar complexity as our method except of the co-occurrence learning step. Given d (downscaling factor in each spatial dimension), our method¹ would require only a little more computation time than [2]. On a different note, we mention that the idea of co-occurrence fairly holds for gray-scale images. However, for downscaling a color image, we need to process each of the three color channels separately.

C. Properties of Co-occurrence Kernel

The co-occurrence kernel h exhibits the following properties:

- 1) Positivity: $h(a, b) \geq 0, \forall(a, b)$.
- 2) Symmetric: $h(a, b) = h(b, a)$.
- 3) Positive definite: For any feasible collection of points $t_i, i = 1, \dots, n$, the Gram matrix with elements $h_{i,j} = h(t_i, t_j)$ is positive definite matrix.

Further, it can also be shown that this co-occurrence kernel satisfy the Cauchy-Schwartz inequality $h^2(a, b) \leq h(a, a)h(b, b)$.

IV. EXPERIMENTAL RESULTS

A. Parameters

In our algorithm, there is only one parameter to control, k . It basically determines the size of the square neighborhood \mathcal{S} while building the similarity matrix in (2). Note that each of the possible pair occurs in the aggregation step in (1) should also be considered during the construction of the co-occurrence matrix in (2). This basic observation leads to $k \geq d$. In a practical scenario of downscaling, the downscaling factor d is a user-defined quantity. Whereas, k is the algorithmic parameter to be set with reference to d . In Figure 1, we present a visual result to demonstrate the effect of various possible k for a fixed d . In this experiment, we used $d = 2$ and $k = \{2, 3, 5\}$.

¹Matlab codes will be shared upon publication.



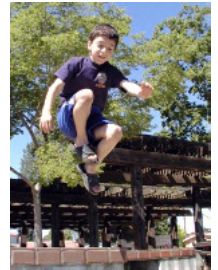
(a) Input.



(b) $k = 2$.



(c) $k = 3$.



(d) $k = 5$.

Fig. 1. Effects of the model parameter k for downscaling factor 2. The input image of (300×400) is downscaled to an image of (150×200) pixels. All the output images are visually very similar.

We notice that all three downscaled images are visually indistinguishable. In other words, the proposed method is less sensitive to k as long as it is at least (or more than) d .

B. Performance on Exhaustive Images

To validate the practical relevance of our proposal, we performed a large number of experiments on an extensive set of images for many different downscaling factor. We also compare with the existing downscaling methods include subsampling, Lanczos filter [7], bi-cubic, Nehab [10], Kopf [14], Oztireli [1], and Weber [2]. In all comparisons with other techniques, the images were either generated using software provided by their own authors or directly downloaded from online repository maintained by the authors. We encourage the readers to take zoom-in on the PDF (full-resolution) for best view (and visual comparisons). The images were obtained from the supplemental/web-page of [14], [2], and [31]. In all the experiments here, we performed uniform downscaling. Therefore, for a reported downscaling factor d , the total

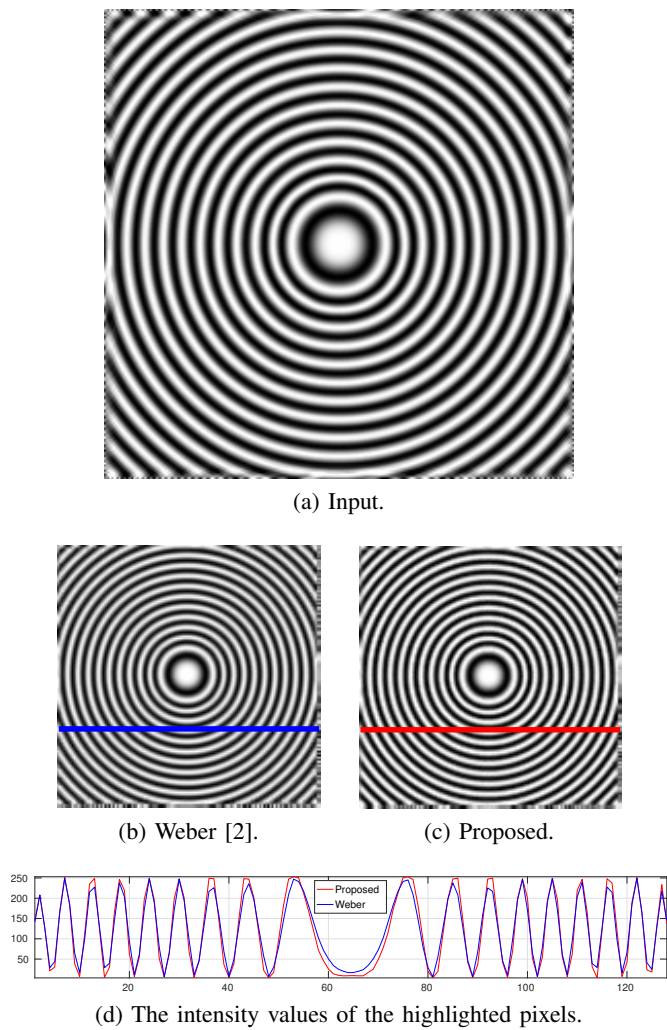


Fig. 2. Downsampling of a radial chirp for a factor $d = 2$. The intensities of the highlighted pixels in both the downsampled images are plotted in Fig. 2(d). Notice that the proposed method can preserve the sharp edges better.

number of pixels is reduced by a factor d^2 . Here we present only a few representative examples. However, we have covered various different types of practical images as follows:

1) *Synthetic image*: An example of downsampling on a synthetic image is shown in Figure 2. Here we compare our method with [2], which was found to be the best (and recent) method as shown in Figure 4. The blue plot in Figure 2(d) is the intensity values of the highlighted pixels in Figure 2(b), obtained using [2]. Similarly, the red plot in Figure 2(d) is the intensity values of the highlighted pixels in Figure 2(c), obtained using our method. We see that the downsampled image using the proposed method exhibits more details than [2]. In fact, it is desired for an efficient downsampling method to successfully retain the visually important high-frequency details.

2) *Painted image*: We show the results of downsampling a hand-drawn portrait of the Italian painter Vittore

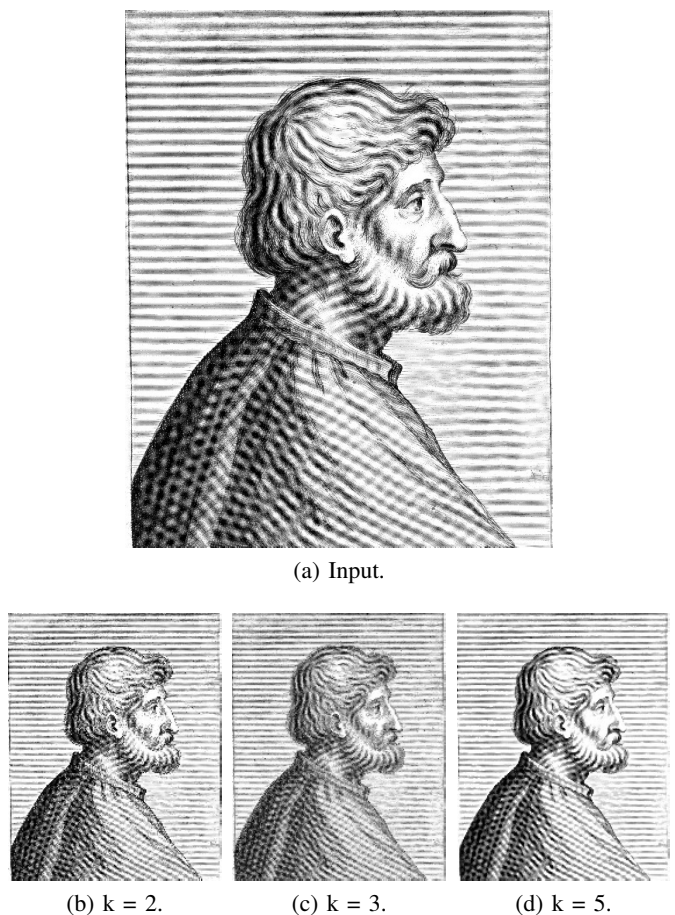


Fig. 3. Downsampling of a hand-drawn portrait for a factor $d = 3$. The output in (d) obtained using the proposed downsampling technique looks most sharper and clear than than the rest two outputs.

Carpaccio in Figure 3. The smaller images in Figure 3(b)-(d) contain (231×184) pixels; whereas the input image has (693×552) pixels. The face in each of the downsampled images is quite instructive. This indicates that there is less blurring in the output of our technique as compared to the rest two methods. In other words, the proposed approach can achieve competitive performance with the existing methods.

3) *Natural image*: We now compare the proposed method with some state-of-the-art methods for downsampling of natural images (both gray-scale and color). One such comparison was already reported in Figure 4. It is evident from the close-ups in Figure 4(b) that the proposed method outperforms the other methods in retaining the fine details which were present in the input image. More comparisons are in Figures 5 and 8.

In Figure 5, we show the results for a gray-scale image. The input image of size (1536×2004) is downsampled to (128×170) pixels. A relatively high downsampling factor $d = 12$ is considered in this experiment. The downsampled image obtained using our technique seems



Fig. 4. Comparison of various image-downscaling techniques. The input image of (512×768) pixels is downscaled to (128×192) pixels with: (c) subsampling, (d) Oztireli [1], (e) bicubic, (f) Weber [2], (g) Lanczos, and (h) proposed method. From the close-ups in (b), it is very evident that the proposed technique outperforms the existing methods. Best viewed at zoomed-in on a computer screen.

to be comparable with the outputs of the other methods. Sometimes, it is not quite clear which image looks visually better. In fact, there is a fundamental tradeoff between the downscaling factor and visual quality of the downsampled image. This phenomenon is applicable to all methods. It usually appears that a downsampled image exhibits similar kind of artifacts which occur in image compression. To evaluate the performance using an objective measure, we use a JPEG image quality (no-reference) metric [33]. A higher value of metric indicates

better image quality. We see that our method performs better in terms of this quality metric.

Figure 8 shows a color image of an outdoor natural scene. In this case, the downscaling factor is 4. We notice that the output of our method looks better than the existing approach. However, similar to the previous example, we also use a no-reference quality measure NIQE [34] to evaluate the performance of the downscaling methods. Among the output of all downscaling approaches in the list, the one obtained using the proposed method has

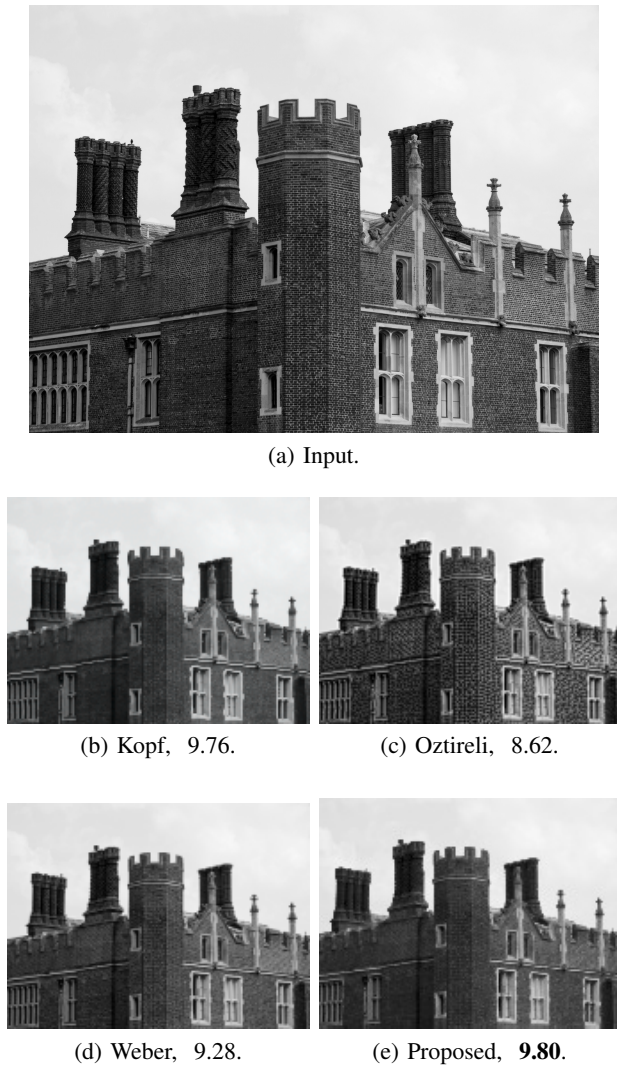


Fig. 5. Downscaling of a gray-scale image for a downscaling factor $d = 12$. A no-reference JPEG quality score [33] is mentioned in the captions of the downscaled images. A higher value of this score represents a better quality.

the least NIQE score; therefore the best downscaling is achieved. We notice in all three figures that our method provides a faithful representation of the input image after the downscaling operation.

4) *Textured image*: Our technique works well for textured images as well. Such an example is shown in Figure 6, where the input image is a mosaic made of tiny pieces. The original image of size (1600×1064) is downscaled to (200×133) pixels. Even for such a high downscaling factor, the output image obtained using our technique is found to exhibit reasonably competitive visual quality as compared to the existing downscaling methods.

5) *Image with high-frequencies*: A typical challenge for most of the downscaling algorithms is to preserve the high-frequency information present in the input image.



Fig. 6. Downscaling of a textured images using various methods. The downscaling factor $d = 8$.

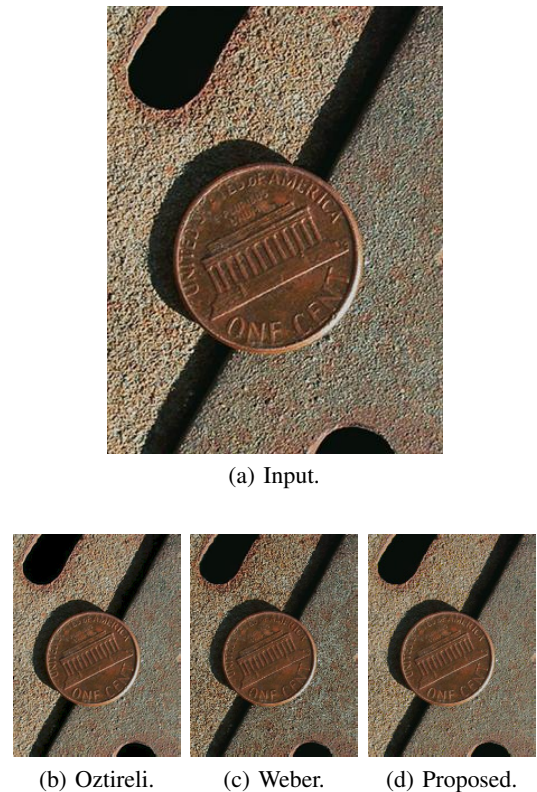


Fig. 7. Downscaling of a *coin* image which contains structured fine details.



(a) Input.



(b) Subsampling, 5.4.



(c) Bicubic, 7.07.



(d) Lanczos, 5.19.



(e) Oztireli, 6.66.



(f) Weber, 4.52.

(g) Proposed, **3.89**.

Fig. 8. Comparison of various image-downscaling techniques. The input image of (704×1024) pixels is downscaled to (176×256) pixels with: (b) subsampling, (c) bicubic, (d) Lanczos, (e) Oztireli [1], (f) Weber [2], and (g) the proposed method. A no-reference quality metric NIQE [34] is mentioned in the captions. A smaller NIQE value represents better image quality. As expected, the input image has the least NIQE value. Among the downscaled images in (b)-(g), the image obtained using the proposed method has the smallest NIQE value. Best viewed at zoomed-in on a computer screen.

To particularly study the performance of our method for this task, we have experimented with the selected images in Figure 7. We downsampled a coin image of size of (400×300) to an image of (200×150) pixels using various techniques. Note that our approach can faithfully retain various forms of high-frequency fine details in both cases.

V. CONCLUSION

In this paper, we proposed a new method for image downscaling. The proposed idea is a special instance

of kernel filtering, where pixel-pair co-occurrence was used as the similarity measure. The co-occurrence feature was directly learned directly from the input image. In a perspective, the proposed feature learning based approach opens up a new direction for learning based downscaling in future. We showed that the proposed image downscaling technique can achieve better performance than existing methods qualitatively as well as quantitatively. Despite of its effective downscaling capacity, it has very simple and parallelizable implementation. The algorithm can be applied to downscale video as well.

REFERENCES

- [1] A Cengiz Öztireli and Markus Gross, "Perceptually based downscaling of images," *ACM Transactions on Graphics (TOG)*, vol. 34, no. 4, pp. 77, 2015.
- [2] Nicolas Weber, Michael Waechter, Sandra C Amend, Stefan Guthe, and Michael Goesele, "Rapid, detail-preserving image downscaling," *ACM Transactions on Graphics (TOG)*, vol. 35, no. 6, pp. 205, 2016.
- [3] Xianxu Hou, Jiang Duan, and Guoping Qiu, "Deep feature consistent deep image transformations: Downscaling, decolorization and hdr tone mapping," *arXiv preprint arXiv:1707.09482*, 2017.
- [4] Faraz Saeedan, Nicolas Weber, Michael Goesele, and Stefan Roth, "Detail-preserving pooling in deep networks," *Proc. IEEE Conference on Computer Vision and Pattern Recognition*, pp. 9108–9116, 2018.
- [5] Heewon Kim, Myungsub Choi, Bee Lim, and Kyoung Mu Lee, "Task-aware image downscaling," *Proceedings of the European Conference on Computer Vision (ECCV)*, pp. 399–414, 2018.
- [6] Claude E Shannon, "Communication in the presence of noise," *Proceedings of the IEEE*, vol. 72, no. 9, pp. 1192–1201, 1984.
- [7] Claude E Duchon, "Lanczos filtering in one and two dimensions," *Journal of Applied Meteorology*, vol. 18, no. 8, pp. 1016–1022, 1979.
- [8] Don P Mitchell and Arun N Netravali, "Reconstruction filters in computer-graphics," in *ACM Siggraph Computer Graphics*, 1988, vol. 22, pp. 221–228.
- [9] Philippe Thévenaz, Thierry Blu, and Michael Unser, "Interpolation revisited [medical images application]," *IEEE Transactions on Medical Imaging*, vol. 19, no. 7, pp. 739–758, 2000.
- [10] Diego Nehab and Hugues Hoppe, "Generalized sampling in computer graphics," *Microsoft Research, Redmond, WA, USA, Tech. Rep. MSR-TR-2011-16*, 2011.
- [11] Matthew Trentacoste, Rafal Mantiuk, and Wolfgang Heidrich, "Blur-aware image downsampling," *Computer Graphics Forum*, vol. 30, no. 2, pp. 573–582, 2011.
- [12] Ramin Samadani, Tim Mauer, David Berfanger, Jim Clark, and Brett Bausk, "Representative image thumbnails: Automatic and manual," *Human Vision and Electronic Imaging XIII*, vol. 6806, pp. 68061D, 2008.
- [13] C. Tomasi and R. Manduchi, "Bilateral filtering for gray and color images," *Proc. IEEE International Conference on Computer Vision*, pp. 839–846, 1998.
- [14] Johannes Kopf, Ariel Shamir, and Pieter Peers, "Content-adaptive image downscaling," *ACM Transactions on Graphics (TOG)*, vol. 32, no. 6, pp. 173, 2013.
- [15] Peyman Milanfar, "A tour of modern image filtering: New insights and methods, both practical and theoretical," *IEEE Signal Processing Magazine*, vol. 30, no. 1, pp. 106–128, 2013.
- [16] Chao-Tsung Huang, "Fast distribution fitting for parameter estimation of range-weighted neighborhood filters," *IEEE Signal Processing Letters*, vol. 23, no. 3, pp. 331–335, 2016.
- [17] Sanjay Ghosh and Kunal N Chaudhury, "Fast and high-quality bilateral filtering using Gauss-Chebyshev approximation," *Proc. International Conference on Signal Processing and Communications*, pp. 1–5, 2016.
- [18] Sanjay Ghosh, Pravin Nair, and Kunal N Chaudhury, "Optimized Fourier bilateral filtering," *IEEE Signal Processing Letters*, vol. 25, no. 10, pp. 1555–1559, 2018.
- [19] Anna Gabiger-Rose, Matthias Kube, Robert Weigel, and Richard Rose, "An FPGA-based fully synchronized design of a bilateral filter for real-time image denoising," *IEEE Transactions on Industrial Electronics*, vol. 61, no. 8, pp. 4093–4104, 2013.
- [20] Sanjay Ghosh and Kunal N Chaudhury, "Artifact reduction for separable nonlocal means," *Journal of Electronic Imaging*, vol. 26, no. 6, pp. 063012, 2017.
- [21] S. Ghosh, R. G. Gavaskar, and K. N. Chaudhury, "Saliency guided image detail enhancement," *Proc. National Conference on Communications (NCC)*, pp. 1–6, 2019.
- [22] Alexander Wong and Jeff Orchard, "A nonlocal-means approach to exemplar-based inpainting," *Proc. IEEE International Conference on Image Processing*, pp. 2600–2603, 2008.
- [23] Sanjay Ghosh and Kunal N Chaudhury, "Color bilateral filtering using stratified fourier sampling," *Proc. IEEE Global Conference on Signal and Information Processing (GlobalSIP)*, pp. 26–30, 2018.
- [24] Sanjay Ghosh and Kunal N Chaudhury, "Fast bright-pass bilateral filtering for low-light enhancement," *Proc. IEEE International Conference on Image Processing (ICIP)*, pp. 205–209, 2019.
- [25] VS Unni, Sanjay Ghosh, and Kunal N Chaudhury, "Linearized admm and fast nonlocal denoising for efficient plug-and-play restoration," *Proc. IEEE Global Conference on Signal and Information Processing (GlobalSIP)*, pp. 11–15, 2018.
- [26] Zhiqiang Zhou, Bo Wang, and Jinlei Ma, "Scale-aware edge-preserving image filtering via iterative global optimization," *IEEE Transactions on Multimedia*, vol. 20, no. 6, pp. 1392–1405, 2017.
- [27] Bill Triggs, "Empirical filter estimation for subpixel interpolation and matching," *Proc. IEEE International Conference on Computer Vision (ICCV)*, vol. 2, pp. 550–557, 2001.
- [28] Azeddine Beghdadi, M-C Larabi, Abdesselam Bouzerdoum, and Khan M Iftekharruddin, "A survey of perceptual image processing methods," *Signal Processing: Image Communication*, vol. 28, no. 8, pp. 811–831, 2013.
- [29] Yongbing Zhang, Debin Zhao, Jian Zhang, Ruiqin Xiong, and Wen Gao, "Interpolation-dependent image downsampling," *IEEE Transactions on Image Processing*, vol. 20, no. 11, pp. 3291–3296, 2011.
- [30] Junjie Liu, Shengfeng He, and Rynson WH Lau, " l_0 -regularized image downscaling," *IEEE Transactions on Image Processing*, vol. 27, no. 3, pp. 1076–1085, 2018.
- [31] Eduardo SL Gastal and Manuel M Oliveira, "Spectral remapping for image downscaling," *ACM Transactions on Graphics (TOG)*, vol. 36, no. 4, pp. 145, 2017.
- [32] Franklin C Crow, "Summed-area tables for texture mapping," *ACM SIGGRAPH Computer Graphics*, vol. 18, no. 3, pp. 207–212, 1984.
- [33] Zhou Wang, Hamid R Sheikh, and Alan C Bovik, "No-reference perceptual quality assessment of jpeg compressed images," *Proc. IEEE International Conference on Image Processing*, vol. 1, pp. I–I, 2002.
- [34] Anish Mittal, Rajiv Soundararajan, and Alan C Bovik, "Making a completely blind image quality analyzer," *IEEE Signal Processing Letters*, vol. 20, no. 3, pp. 209–212, 2013.